Fibers and Polymers 2017, Vol.18, No.5, 965-970
DOI 10.1007/s12221-017-1131-8

ISSN 1229-9197 (print version)
ISSN 1875-0052 (electronic version)

Improvement of High-velocity Impact Properties of Anisogrid Stiffened Composites by Multi-walled Carbon Nanotubes

Reza Eslami-Farsani* and Alireza Shahrabi-Farahani

Faculty of Materials Science and Engineering, K. N. Toosi University of Technology, Tehran 1999143344, Iran
(Received November 20, 2016; Accepted March 24, 2017)

Abstract: The present study represents the influence of adding different weight fractions (0, 0.1, 0.25 and 0.4 wt.%) of multi-walled carbon nanotubes (MWCNT) on the high velocity impact behavior of anisogrid stiffened composite (AGSC) plates. AGSC plates were fabricated through hand lay-up method where E-glass woven fabrics and unidirectional carbon fiber rovings were used as fibrous reinforcement of ribs and skin, respectively. High velocity impact test was performed on these plates by cylindrical projectile with conical nose. Obtained results revealed that the maximum improvement of the high velocity impact properties of AGSC plates were obtained through addition of 0.4 wt.% of MWCNTs. Field emission scanning electron microscopy (FESEM) examinations of the fracture surfaces clearly indicated the improvement in the interfacial adhesion between the fibers and epoxy matrix in the case of the nanocomposite specimens. Also, it was observed that the addition of MWCNTs to the AGSC specimens led to reduce the damage area and increased the damage tolerance, considerably.

Keywords: Anisogrid stiffened composite plates, Multi-walled carbon nanotubes, High velocity impact properties, Energy absorption, Damage area

Introduction

Since the advent of composite materials influence of these materials in various industries due to their unique properties is undeniable. In industrial products, there is a tendency to use the materials that despite being lightweight have high strength and stiffness. In other words, they should have high specific strength and stiffness which led to the development of composite materials [1-5]. Among the various composite structures, grid composite structures have excellence properties such as high specific strength and stiffness, higher energy absorption capability and corrosion resistance. For this purpose they are widely used in aerospace applications such as launch vehicle payload fairing, interstage ring, engine ducting, and for load bearing structures of satellite [6-10].

These structures include a system of ribs that are visually similar to the structures that are meshed with beams or frames. These structures can be involved no outer shell or supported with skin from one side or both sides [11,12]. In these structures, the ribs are the main load bearing elements which have a unidirectional structure [13]. Using the ribs significantly increases the load bearing capacity of the structure without much increment in the structure weight [14]. The anisogrid lattice concept is characterized by a relatively dense system of intersecting diagonal and transverse ribs forming a regular pattern of hexagonal or triangular cells [15,16].

Due to their sensitive usages in aerospace industries, they experience different loading condition such as impact phenomena by foreign objects. Therefore, the study of their behavior under impact loading is an important issue. In recent years, several studies have been conducted about the effects of different nanofillers on the mechanical properties of fiber-reinforced polymer composite materials. Using the nanofillers as reinforcement for polymer composites has a significant effect on their mechanical properties [17-20]. It should be noted that nanofillers do not cause significant changes in the weight of the structures. Rahman *et al.* [21] investigated the reinforcing effect of MWCNTs that functionalized with amine groups on the ballistic behavior of glass fiber/epoxy composites. They reported that with the addition of 0.3 wt.% of MWCNTs, ballistic limit velocity of glass fiber/epoxy composites increased by 6 % in comparison with specimens without MWCNTs. Ferreira *et al.* [22] showed that with the addition of 0.5 wt.% of MWCNTs, absorbed energy of glass fiber/epoxy composites during low velocity impact increased by 18 % compared with control composites.

Obradovic *et al.* [23] reported that the impact absorbed energy of the kolon fiber/polyvinyl butyral composites filled with 1 wt.% of MWCNTs was higher by 73 % compared to the reference composites. Boddu *et al.* [24] found that with the growth of MWCNTs on the surface of glass fibers the ballistic limit velocity of glass fiber/Polyethylene composites was increased by 11.1 % in comparison with composites without MWCNT addition. Mohan *et al.* [25] reported an increase of 42 % in ballistic limit velocity of glass fiber/ epoxy composites with 5 wt.% of nanoclay addition. In the work of Pol *et al.* [26] the highest absorbed energy of glass fiber/epoxy composites was achieved via addition of 5 wt.% of nanoclay.

Most researches associated with GSC structures were focused on the geometry optimization. But besides the design requirements to improve the performance of grid composite

*Corresponding author: eslami@kntu.ac.ir

structures, microstructural modification of them is required. So in the current study, the influence of MWCNTs on the high-velocity impact behavior of AGSC plates was investigated. The epoxy/MWCNTs with various MWCNTs loadings (0, 0.1, 0.25 and 0.4 wt.%) were used as the matrix material for fabrication of ribs and skin of AGSC plates. The obtained results were then used to determine the high velocity impact properties of the plates.

Experimental

Raw Materials

The epoxy resin ML-506 (Bisphenol F) and the curing agent HA-11 (polyamine hardener) were purchased from Mokarrar Engineering Co., Iran. Carboxyl functionalized MWCNTs (COOH-MWCNTs) were supplied by Cheap Tube Co., USA. The properties of purchased MWCNTs are shown in Table 1. Plain weave E-glass fibers with an areal density of 400 g/m^2 supplied by Lintex, China, were used as reinforcement in skin part. Unidirectional carbon fibers (UCF) with average diameter of 7.6 μm and density of 1.76 g/cm^3 were used as reinforcement of ribs.

Preparation of Matrix

MWCNTs with different weight percentage (0, 0.1, 0.25 and 0.4 wt.%) relative to the total weight of the matrix (include resin and hardener) were added into the epoxy resin. To ensure the uniform distribution of MWCNTs in epoxy resin, the mixture was stirred with using a high speed mechanical stirrer at rotational speed of 2000 rpm for 20 min. Then the mixture was sonicated using a probe sonicator at 120 W and 30 % duty cycle. In order to remove air bubbles, the mixture was degassed under vacuum conditions. Finally, curing agent with a weight ratio of 100: 15 was added to the mixture.

Preparation of AGSC Specimens

In this research, silicone molds were used to fabricate the AGSC plates. The specimens were prepared using a hand lay-up method. At first, UCF were impregnated with the epoxy resin that modified MWCNTs and then inserted into the grooves of mold layer by layer to form the skeleton of the ribs. In the next step, laying up the skin using E-glass woven fabrics was performed. Fabricated specimen was held in the room temperature for 3 hours until curing process of resin was accomplished. According to the supplier, In order to attain the highest strength and ultimate curing, specimens were placed at room temperature for 7 days. The fabricated specimens are shown in Figure 1. The specimens were characterized by a length of 150 mm, width of 125 mm and skin thickness of 1.8 mm. The volume fraction of fiber reinforcement in ribs and skin parts were calculated approximately 30 % and 48 %, respectively, for all specimens.

Table 1. Details of the MWCNTs

Diameter (nm)	Length (μm)	Purity (%)	COOH content (wt.%)	Specific surface area (m^2/g)
10-20	10-30	95	2	233

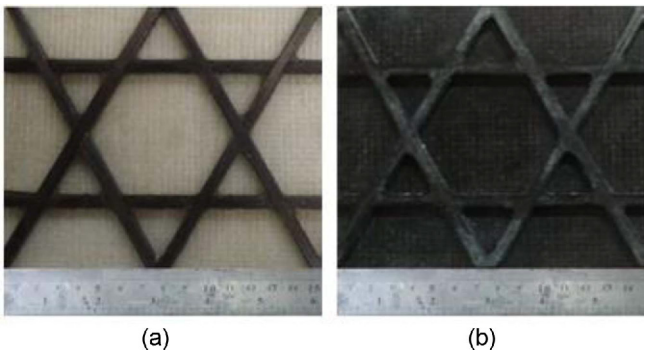

Figure 1. AGSC plates, (a) without MWCNTs and (b) reinforced with MWCNTs.

High-velocity Impact Test

High velocity impact tests were carried out using a gas-gun test set-up. During the tests, both the initial velocity and residual velocity of projectile were recorded. The projectile used for impact tests was cone-shaped that made of Al-7075 alloy with 30 mm in length, 27 g in mass and 21 mm in diameter, as shown in Figure 2. To ensure the test results, each experiment was repeated at least 3 times. Impact velocity was 107 m/s. Both the initial velocity and residual velocity of projectile were recorded.

In the present study, energy absorption with accordance to equation (1) was determined by difference of initial kinetic energy before impact and residual kinetic energy after impact. As well as, the ballistic limit velocity was determined by equation (2).

$$E_a = \frac{1}{2} m_p (V_i^2 - V_r^2) \quad (1)$$

$$V_b = \sqrt{V_i^2 - V_r^2} \quad (2)$$

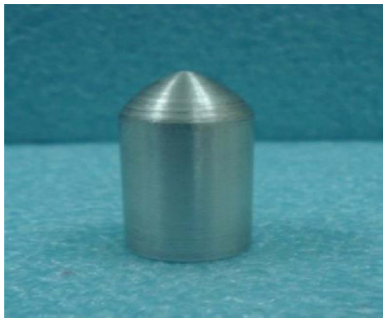

Figure 2. Cone-shaped projectile used in this study.

In the above equations, m_p, V_i and V_r are mass, initial and residual velocity of projectile, respectively. V_b is the ballistic limit velocity and E_a is the energy absorption by the plates.

Analysis of the Fracture Surface

In order to examine the microstructure of the fracture surface, field emission scanning electron microscopy (Mira 3-XMU, 25 kV) was used. In order to increase the conductivity, the specimen's surface was coated with a thin gold layer.

Results and Discussion

Ballistic Limit Velocity and Energy Absorption

Summary of high velocity impact test results on AGSC and unstiffened plates are shown in Table 2. Regardless of effect of MWCNTs, during penetration of projectile into the unstiffened composite plates, the value of energy absorption was 59.3 J. While with reinforcement of composite plate by unidirectional network of ribs, the energy absorption significantly increased and this value was 72.41 J. The presence of unidirectional ribs that reinforced with carbon fibers led to increase the stiffness and strength of AGSC plates and showed more resistance against the stress caused by high velocity impact. As a result spread out of the cracks in different parts of the specimens was difficult and consequently damage tolerance and energy absorption of the plates were improved.

High-velocity impact properties of AGSC plates for various weight fractions of MWCNTs are presented in Figure 3. According to this figure, addition of MWCNTs to the AGSC specimens affected the high velocity impact properties of the resultant plates. The value of ballistic limit velocity for AGSC plates without MWCNTs was 73.24 m/s. While with the addition of 0.4 wt.% of MWCNTs, the amount of ballistic limit velocity was increased to the 80.92 m/s. Which in this case ballistic limit velocity increased by 11 %. Also the amounts of energy absorption for specimens without MWCNTs and reinforced with 0.4 wt.% of MWCNTs were 72.41 and 88.39 J, respectively.

High velocity impact properties of composite materials are highly dependent on the fracture toughness, modulus, tensile strength and fracture strain the fiber and matrix, as well as the interface between the field and fibers [26,27]. One of the factors that improve the high velocity impact properties is

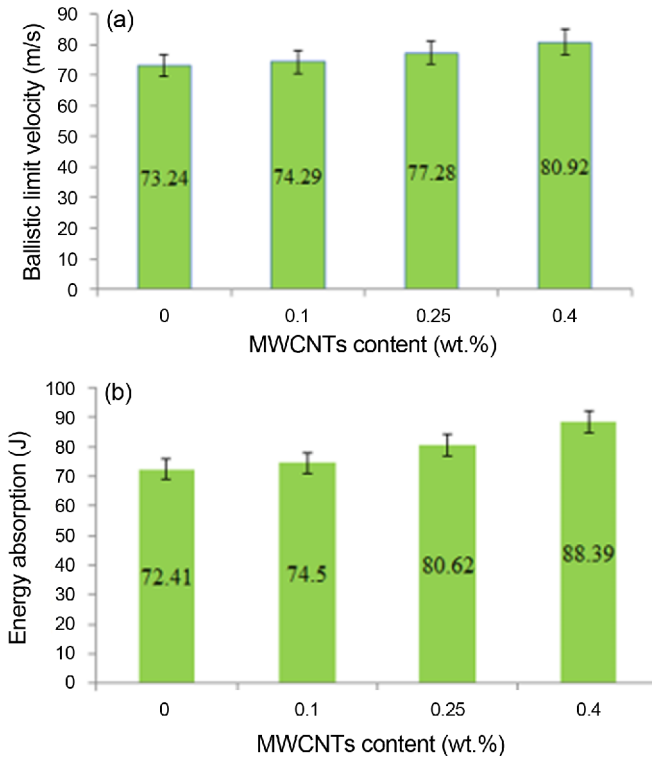

Figure 3. Results of ballistic impact test; (a) ballistic limit velocity and (b) energy absorption of AGSC plates containing varied weight fractions of MWCNTs.

the increment of the stress transfer between the polymer matrix and MWCNTs. In fibrous composites, interface between matrix and fibers has special significance because the applied load is transferred through the interface. In fact interface of matrix and fibers plays an important role in the properties of composite materials. With the introduction of MWCNTs into the epoxy matrix, adherence between matrix and reinforcement fiber was improved. For this reason, effective stress transfer between matrix and fibers was created. As a result, high velocity impact properties of specimens containing MWCNTs were higher than controls specimens [28-31].

On the other hand, MWCNTs by bridging mechanism delay the crack propagation within the matrix and fiber-matrix interface that enhance the fracture toughness of

Table 2. Results of high velocity impact test

Composite type	MWCNTs content (wt.%)	Initial velocity (m/s)	Residual velocity (m/s)	Ballistic limit (m/s)	Absorbed energy (J)	Damaged area (mm^2)
Unstiffened	0	107	84	66.27	59.3	3846.5
AGSC	0	107	78	73.24	72.41	1268.59
AGSC	0.1	107	77	74.29	74.5	1203.18
AGSC	0.25	107	74	77.28	80.62	1041.23
AGSC	0.4	107	70	80.92	88.39	816.95

composites. Due to this phenomenon, to spread out of the cracks more energy is required and the energy absorption of AGSC specimens containing MWCNTs was increased [32-35].

Evaluation of Damaged Area

The main mechanisms of energy absorption due to penetration of cone-shaped projectile in to the AGSC target were fiber breakage, delamination, matrix cracking and perforation. Fiber breakage caused by tensile stress which the applied strain to the fibers is higher than ultimate tensile strain. Matrix cracking is the first failure mode in composite materials which is caused by cracking of matrix along the fibers [36].

Delamination is one of the most important damages in fiber-reinforced composites that caused by interlaminar shear stresses. Delamination in composite structures led to a sharp drop in their load-bearing capacity [37]. Perforation of the specimens is macroscopic failure mode of AGSC plates under high velocity impact and occurs when fiber breakage due to the penetration of the projectile reaches a critical value. As a result projectile completely penetrates into the target [38].

In Figure 4 damaged area of unstiffened and AGSC plates reinforced with MWCNTs are shown. For unstiffened plates after penetration of projectile, damage was created in a wide range of composite. While for AGSC plates contain network of unidirectional ribs, less damage was created. In fact presence of the ribs due to their high stiffness and strength prevent the propagation of cracks in other parts of AGSC plate. Also the skeleton of the ribs was not damaged because of the unidirectional nature of the network of ribs which separation of the ribs from skin didn't occur easily. Generally, the ribs in GSC structures act as elastic supports and prevent the crack spread of cracks from one cell to adjacent cell as well as reduced the damage area of specimens.

Also with the addition of MWCNTs, the damage size of AGSC plates compared to the control specimens was significantly decreased. For specimens without MWCNTs, damaged area was 1268.59 mm^2. While with introduction of 0.4 wt.% of MWCNTs was decreased to the value of 816.95 mm^2. This decrement in damaged area was due to this fact that the addition of MWCNTs increased the stiffness of AGSC plates and absorbed more applied energy by elastic deformation compared to the control specimens. Therefore, the energy is required to create damage is increased which causes the reduction in damage area. On the other hand by adding MWCNTs resistance to delamination due to improvement of interface between matrix and fibers, resistance to delamination was increased. In fact in specimens containing MWCNTs less delamination occurred. As a result, the damage area of composites was decreased.

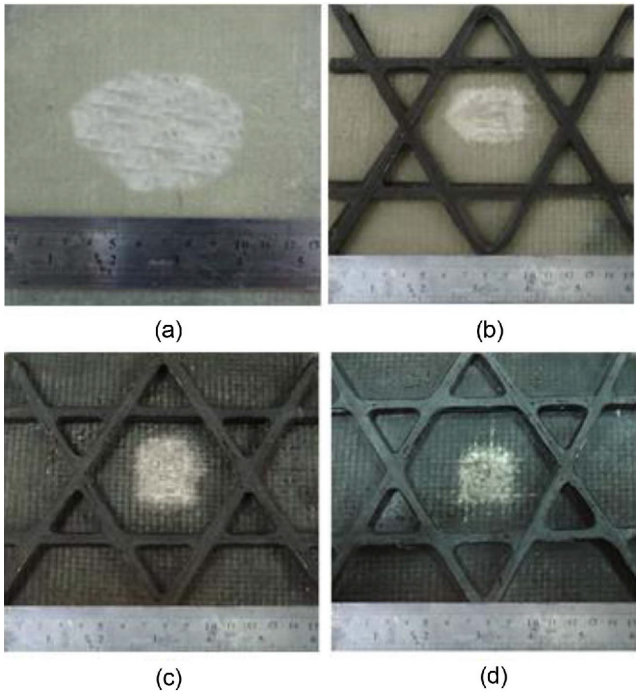

Figure 4. Damage area of (a) unstiffened plates and AGSC plates reinforced with (b) 0 wt.%, (c) 0.25 wt.%, and (d) 0.4 wt.% of MWCNTs.

Microstructural Analysis

In Figure 5, the adhesion between fiber and matrix has

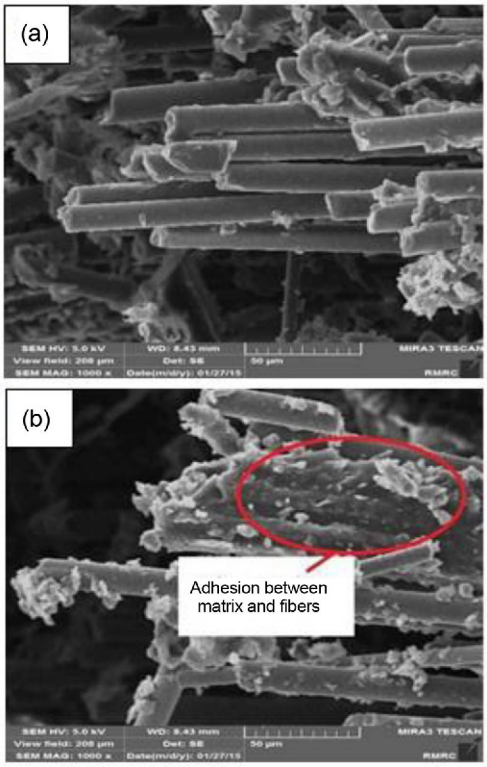

Figure 5. FESEM images taken from fracture surface of AGSC plates; (a) without MWCNTs and (b) containing MWCNTs.

been investigated. For specimens without MWCNTs (Figure 5(a)), matrix is entirely separated from the surface of fibers and fiber surface is clean due to weak adhesion between matrix and fibers. Contrary for the specimens containing MWCNTs (Figure 5(b)), matrix is attached to the fibers which reflect the improvement of adhesion between matrix and fibers in the presence of MWCNTs.

Figure 6 presents the fracture surface of the matrix without MWCNTs and reinforced with MWCNTs. As can be seen, the fracture surface of specimens containing MWCNTs (Figure 6(b)) is rougher than the neat epoxy resin because of the addition of MWCNTs into the polymer matrix which shows that the spread of cracks in the presence of MWCNTs has been more difficult. The crack bridging process is idealized as normal MWCNTs pullout from the polymer matrix which is shown in Figure 7.

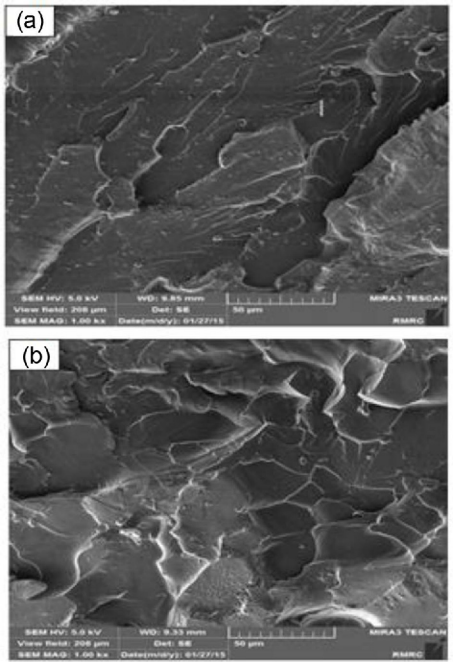

Figure 6. FESEM images taken from matrix (a) without MWCNTs and (b) containing MWCNTs.

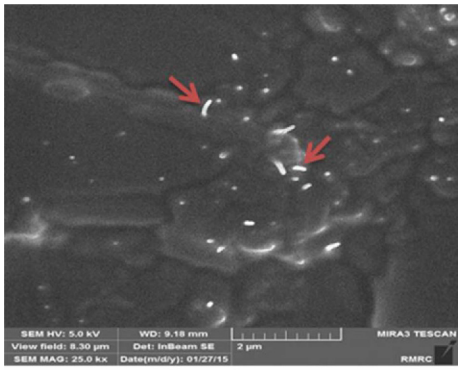

Figure 7. MWCNTs pull out in the matrix.

Conclusion

In this study, improvement of high velocity impact properties of anisogrid stiffened composite plates by the addition of MWCNTs was investigated. Various weight fractions of MWCNTs (0, 0.1, 0.25 and 0.4 wt.%) was incorporated into the matrix. Experimental results are as follows:

1. Comparing high velocity impact test results of unstiffened composite plates and anisogrid composite plates indicated that the presence of network of ribs act as a barrier against the propagation of cracks which led to increase the energy absorption and damage tolerance of the anisogrid composite specimens.
2. With the addition of 0.4 wt.% of MWCNTs, ballistic limit and energy absorption of anisogrid stiffened composite plates increased by 11 % and 22 % in comparison with specimens without MWCNTs, respectively.
3. Improvement of high velocity impact properties with the addition of MWCNTs was due to improvement in the interfacial properties and effective load transfer from resin matrix to fibers.
4. The most important mechanisms of energy absorption during high velocity impact are fiber breakage, matrix cracking and delamination.
5. With introduction of MWCNTs, Damage size of anisogrid composite plates was considerably decreased.

References

1. H. Ebrahimnezhad-Khaljiri and R. Eslami-Farsani, *Fiber. Polym.*, **16**, 2445 (2015).
2. H. Kanou, S. M. Nabavi, and J. Eskandari-Jam, *Int. J. Eng. Sci. Tech.*, **5**, 42 (2013).
3. J. Eskandari-Jam, M. Noorabadi, H. Taghavian, M. Mohammadi, and N. Namdaran, *Res. Appl. Mech. Eng.*, **1**, 5 (2012).
4. E. V. Morozov and A. V. Lopatin, *Compos. Struct.*, **93**, 1640 (2011).
5. M. Moeinifarda, G. H. Liaghat, G. H. Rahimi, A. Talezadehlari, and H. Hadavini, *Compos. Struct.*, **152**, 626 (2016).
6. V. V. Vasiliev, V. A. Barynin, and A. F. Razin, *Compos. Struct.*, **94**, 1117 (2012).
7. V. V. Vasiliev and A. F. Razin, *Compos. Struct.*, **76**, 182 (2006).
8. Q. Huang, M. Ren, and H. Chen, *Appl. Compos. Mater.*, **20**, 303 (2013).
9. S. Yazdani and G. H. Rahimi, *Sci. Res. Ess.*, **8**, 902 (2013).
10. D. Wang and M. M. Abdalla, *Compos. Struct.*, **119**, 767 (2015).
11. K. Lim, W. He, and Z. Guan, *Adv. Mater. Res.*, **875**, 755 (2014).
12. E. Wodesenbet, S. Kidane, and S. S. Pang, *Compos. Struct.*, **60**, 159 (2003).

13. G. Li and J. Cheng, *J. Compos. Mater.*, **41**, 2939 (2007).
14. G. Totaro, *Compos. Struct.*, **129**, 101 (2015).
15. G. Totaro, *Compos. Struct.*, **95**, 403 (2013).
16. F. Sun, H. Fan, C. Zhou, and D. Fang, *Compos. Struct.*, **101**, 180 (2013).
17. S. Zainuddin, A. Fahim, T. Arifin, M. V. Hosur, M. M. Rahman, J. D. Tyson, and S. Jeelani, *Compos. Struct.*, **110**, 39 (2014).
18. M. H. Pol and G. H. Liaghat, *Polym. Compos.*, **37**, 1173 (2016).
19. D. K. Rathore, R. K. Prusty, D. S. Kumar, and B. C. Ray, *Compos. Pt. A-Appl. Sci. Manuf.*, **84**, 364 (2016).
20. P. Panse, A. Anand, V. Murkute, A. Ecka, R. Harshe, and M. Joshi, *Polym. Compos.*, **37**, 975 (2016).
21. M. Rahman, M. Hosur, S. Zainuddin, U. Vaidya, A. Tauhid, A. Kumar, J. Trovillion, and S. Jeelani, *Int. J. Impact. Eng.*, **57**, 108 (2013).
22. J. A. M. Ferreira, D. S. C. Santos, C. Capela, and J. D. M. Costa, *Fiber. Polym.*, **16**, 173 (2015).
23. V. Obradovic, D. B. Stojanovic, I. Zivkovic, V. Radojevic, P. S. Uskokovic, and R. Aleksic, *Fiber. Polym.*, **16**, 138 (2015).
24. M. V. Boddu, M. W. Brenner, J. S. Patel, A. Kumar, P. R. Mantena, T. Tadepalli, and B. Pramanik, *Compos. Pt. B-Eng.*, **88**, 44 (2016).
25. T. P. Mohan, R. Velmurugan, and K. Kanny, *Compos. Pt. B-Eng.*, **82**, 178 (2015).
26. M. H. Pol, G. H. Liaghat, and F. Hajiarazi, *J. Compos. Mater.*, **47**, 1563 (2013).
27. K. Peng, Y. J. Wan, D. Y. Ren, Q. W. Zeng, and L. C. Tang, *Fiber. Polym.*, **15**, 1242 (2014).
28. S. Aziz, S. A. Rashid, S. Rahmanian, and M. A. Salleh, *Polym. Compos.*, **36**, 1941 (2015).
29. Z. Wu, L. Meng, L. Liu, Z. Jiang, L. Xing, D. Jiang, and Y. Huang, *Fiber. Polym.*, **15**, 659 (2014).
30. M. S. Islam, Y. Deng, L. Tong, S. N. Faisal, A. K. Roy, A. I. Minett, and V. G. Gomes, *Carbon*, **96**, 701 (2016).
31. F. L. Shan, Y .Z. Gu, M. Li, Y. N. Liu, and Z. G. Zhang, *Polym. Compos*., **34**, 41 (2013).
32. B. T. Marouf, Y. W. Mai, and R. Bagheri, *Polym. Rev.*, **56**, 70 (2016).
33. A. Patra and N. Mitra, *Compos. Sci. Tech.*, **101**, 94 (2014).
34. J. A. M. Ferreira, D. S. C. Santos, C. Capela, and J. D. M. Costa, *Fiber. Polym*., **16**, 173 (2015).
35. J. S. Fenner and I. M. Daniel, *Compos. Pt. A-Appl. Sci. Manuf.,* **65**, 47 (2014).
36. N. Razali, M. T. H. Sultan, F. Mustapha, N. Yirdis, and M. R. Ishak, *Int. J. Eng. Sci.*, **3**, 8 (2014).
37. N. S. S. Nair, C. V. V. Kumar, N. K. K. Naik, and S. Shaktivesh, *Mater. Des.*, **51**, 833 (2013).
38. P. Udatha, C. V. S. Kumar, S. N. Nair, and N. K. Naik, *J. Strain. Anal. Eng. Des.*, **47**, 419 (2012).